Volume 12 | Number 20 | 28 May 2014 | Pages 3139–3312

Organic & Biomolecular Chemistry

www.rsc.org/obc

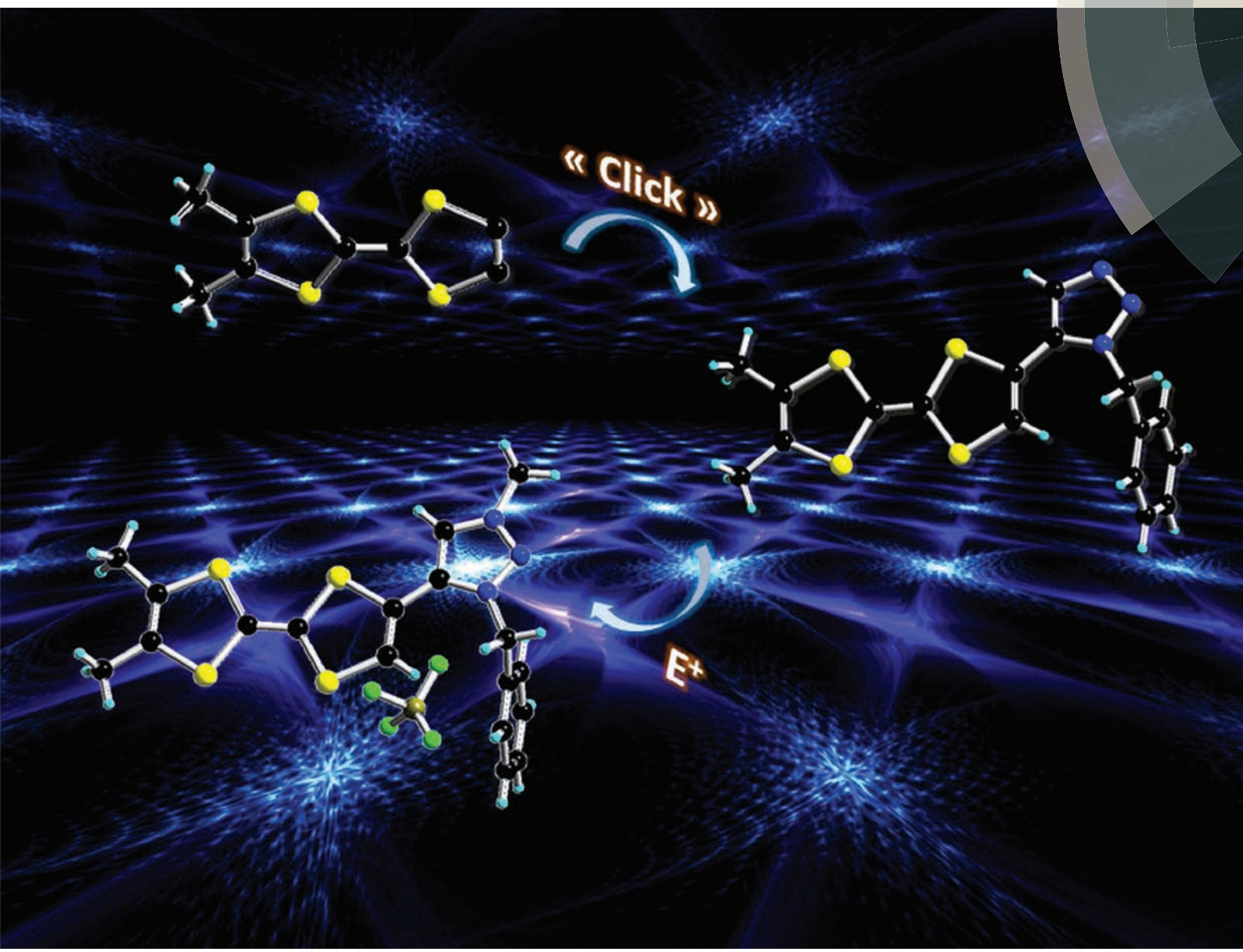

ISSN 1477-0520

ROYAL SOCIETY OF CHEMISTRY

PAPER

Thomas Biet and Narcis Avarvari

Tetrathiafulvalene mono- and bis-1,2,3-triazole precursors by click chemistry: structural diversity and reactivity

Organic & Biomolecular Chemistry

PAPER

View Article Online
View Journal | View Issue

Cite this: *Org. Biomol. Chem.*, 2014, **12**, 3167

Tetrathiafulvalene mono- and bis-1,2,3-triazole precursors by click chemistry: structural diversity and reactivity†

Thomas Biet and Narcis Avarvari*

Received 20th January 2014,
Accepted 14th February 2014

DOI: 10.1039/c4ob00148f

www.rsc.org/obc

The donor *ortho*-dimethyl-TTF-(*N*-*n*-Bu-1,2,3-triazole) 1,5-isomer has been synthesized by click chemistry following a ruthenium-catalyzed azide–alkyne cycloaddition procedure. The single crystal X-ray analysis showed a planar conformation between the TTF and triazole units and a set of intermolecular interactions at the supramolecular level in the solid state. The same procedure allowed the preparation of the corresponding *ortho*-dimethyl-TTF-bis(triazole) which was also structurally characterized. Because of the steric hindrance, the triazole units are no longer planar with the TTF backbone. The reactivity of the triazole ring has been investigated in protonation and alkylation reactions, monitored by UV-visible spectroscopy, which clearly showed the red shift of the intramolecular charge transfer band. A TTF-methyl-triazolium salt has been isolated and analyzed by single crystal X-ray analysis. All of the TTF-triazoles and triazolium salts are valuable precursors for radical cation salts due to their oxidation potentials and variety of possible intermolecular interactions.

Introduction

Synthetic methods based on click chemistry strategies have developed increasingly over the last decade,[1] with one of the most useful reactions being the copper-catalyzed azide–alkyne cycloaddition (CuAAC) that allows the straightforward preparation of 1,2,3-triazoles (1,4-isomers).[2] These heterocycles have proved to be useful units in chemical sensing[3] and peptidomimetic research,[4] and are also interesting ligands towards transition metals.[5] Alternatively, the 1,5-isomers of 1,2,3-triazoles have been efficiently prepared by the azide–alkyne cycloaddition mediated by a ruthenium(II)-based catalyst.[6] We have recently employed both strategies for the synthesis of the new electroactive ligands TTF-1,2,3-triazoles as 1,4- and 1,5-isomers (Scheme 1),[7] respectively, where the electroactive part is represented by the TTF (tetrathiafulvalene) unit, and in which TTF and triazoles are directly connected. A large difference in their electrochemical behavior was observed, *e.g.* much easier oxidation for the 1,4-isomers than for the 1,5-isomers, and, accordingly, in their relative kinetic stability. Moreover, coordination of the more stable 1,5-isomers to $Cu(hfac)_2$ (hfac = hexafluoroacetylacetonate) fragments induced an unusual cathodic shift of the oxidation potentials of TTF.

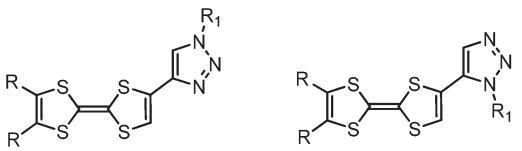

Scheme 1 TTF-1,2,3-triazoles.

In the other few published examples of TTF-triazole systems, with linkers of various lengths between TTF and triazole,[8] the latter serves mainly to connect other electroactive moieties to TTF, such as perylene diimide[9] or ferrocene.[10] From a general point of view, the association of TTF with coordinating groups within electroactive ligands[11] represents a powerful strategy to access either multifunctional molecular materials, in which a combination of different physical properties can be achieved,[12] or electroactive catalysts.[13] In this respect, nitrogen-containing five-membered rings, such as oxazolines,[14] pyrazoles[15] or imidazoles[16] have been attached to TTF, while the synthesis and coordination chemistry of TTF-triazole ligands has been reported much more recently.[7] Beside their use as ligands, the basicity and nucleophilicity of the triazole ring should in principle allow for the modulation of the intramolecular charge transfer and the electrodonating

Laboratoire MOLTECH-Anjou, Université d'Angers, CNRS, UMR 6200, UFR Sciences, Bât. K, 2 Bd. Lavoisier, 49045 Angers, France. E-mail: narcis.avarvari@univ-angers.fr; Fax: (+33)02 41 73 54 05; Tel: (+33)0241 73 50 84

†Electronic supplementary information (ESI) available. CCDC 982420–982423. For ESI and crystallographic data in CIF or other electronic format see DOI: 10.1039/c4ob00148f

character of TTF upon protonation or reaction with electrophiles.[16b] Moreover, the versatility of the two "click" strategies, *i.e.* Cu *versus* Ru catalysis, guarantees the preparation of a whole library of TTF-triazoles by the appropriate choice of the acetylene and azide units. The substitution pattern, type of isomers, *i.e.* 1,4-*versus* 1,5-, and number of triazole units should have an important influence not only on the electrochemical properties and coordination ability, but also on the supramolecular architectures in crystals, which ultimately determines the solid state properties of the derived materials. We report herein the synthesis, reactivity and solid state structures of TTF-mono and -bis(1,2,3-triazoles), together with those of a TTF-triazolium salt.

Results and discussion

The TTF-triazole **1** (Schemes 1 and 2), with Me groups on TTF and a benzyl (Bn) substituent on the nitrogen atom N1, was synthesized as previously described by a Ru-catalyzed azide–alkyne cycloaddition (RuAAC) reaction between the dimethyl-TTF-acetylene and benzyl azide.[7] In order to evaluate the influence of different substituents on the triazole ring, the ligand TTF-triazole **2** with an *n*-butyl (*n*-Bu) group instead of Bn was prepared following the same procedure by using *n*-butyl azide (Scheme 2).

The donor *ortho*-dimethyl-TTF **3** is well suited for a selective bis-functionalization, allowing us to attempt the preparation of TTF-bis(triazoles) through both strategies. Accordingly, the diiodo derivative **4** has been prepared upon the double lithiation of **3** followed by treatment with perfluorohexyl iodide. Then, a double Sonogashira coupling under classical conditions with trimethylsilyl acetylene afforded the bis(acetylenic) compound **5** which was further deprotected in the presence of $(n\text{-Bu})_4$NF. The resulting TTF-bis(acetylene) **6** was then rapidly engaged in a double cycloaddition reaction with benzyl azide following either the copper or the ruthenium-based catalysis (Scheme 3).

While in the case of the Ru-catalyzed reaction the TTF-bis(triazole) **8** was obtained in low yield (15%) as the bis(1,5-isomer), the Cu-based catalysis afforded only the TTF-triazole-acetylene **7** as the 1,4-isomer in even lower yield (10%) with no trace of the bis(triazole). The low yields are very likely attributed to the sensitivity of the TTF-diacetylene **6** which partially degrades under the reaction conditions. Moreover, as previously mentioned, the 1,4-isomers are less stable than the 1,5-isomers,[7] therefore compound **7**, which is an intermediate towards the desired bis(triazole), degrades before the second acetylene unit reacts in the cycloaddition reaction. Nevertheless, a small amount of **7** could be purified by column chromatography and characterized by ^{1}H NMR and mass spectrometry, yet the compound has a limited stability in air even in the solid state.

Cyclic voltammetry measurements (see ESI†) show that the oxidation potentials for the donor **2**, of 0.45 and 0.85 V *versus* SCE for $E^1_{1/2}$ and $E^2_{1/2}$ respectively, are identical to those for the benzyl derivative **1**. In the case of the bis(triazole) **8**, anodic shifts of 0.13 and 0.11 V for the first and second oxidation processes are observed when compared to the mono(triazole) **1** (*e.g.* $E^1_{1/2}$ = 0.44 V (**1**) and 0.57 V (**8**), $E^2_{1/2}$ = 0.85 V (**1**) and 0.96 V (**8**)), thus evidencing the withdrawing effect of the triazole ring when connected to TTF as the 1,5-isomer.

The solid state structures of the mono(triazole) **2**, bis(triazole) **8**, as well as the intermediate **5** (see ESI†), have been determined by single crystal X-ray diffraction analysis.

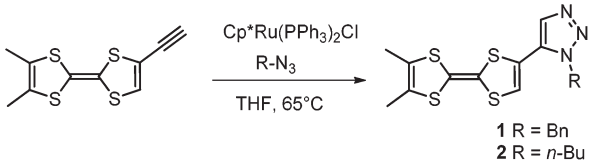

Scheme 2 Synthesis of the TTF-mono(triazoles) **1** and **2**.

The crystal structure of 1-butyl-5-(*ortho*-dimethyl-TTF)-1,2,3-triazole (2)

The solid state structure of the benzyl derivative **1**, previously described,[7] shows quasi-planarity between the TTF and triazole units, with a dihedral angle of 6.0° and the s-*trans* conformation, and the existence of short intermolecular S···S contacts. In the case of **2**, suitable crystals, as orange needles, for X-ray analysis were obtained by the slow evaporation of the

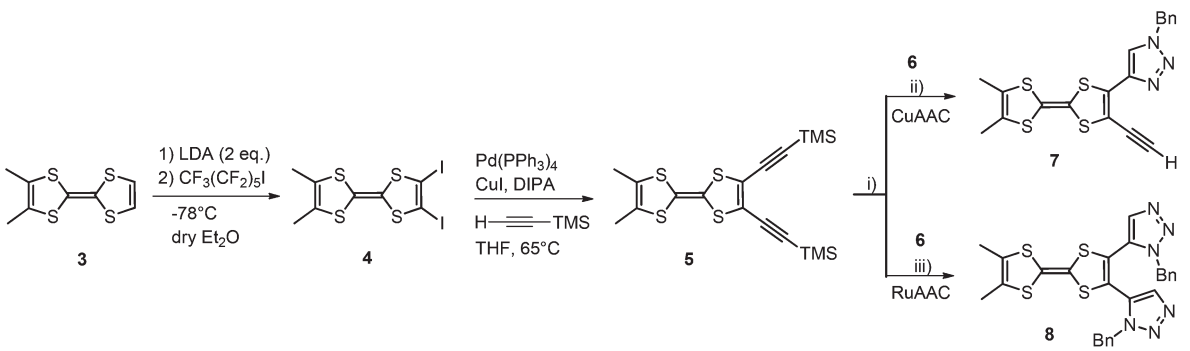

Scheme 3 Synthesis of **7** and **8**. Reaction conditions: (i) $(n\text{-Bu})_4$NF, THF–MeOH (1 : 1); (ii) CuI, $PhCH_2N_3$, $CHCl_3$–DIPEA (1 : 1), 65 °C; (iii) Cp*RuCl-$(PPh_3)_2$, $PhCH_2N_3$, THF, 65 °C.

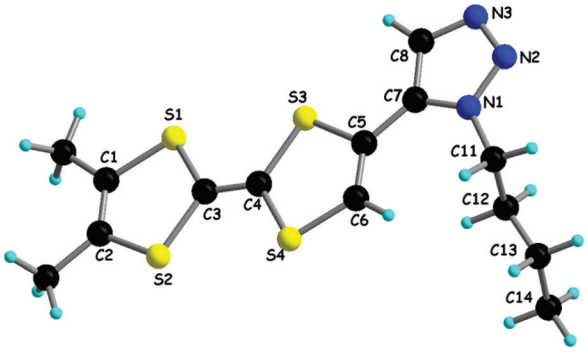

Fig. 1 Molecular structure of **2** along with the numbering scheme.

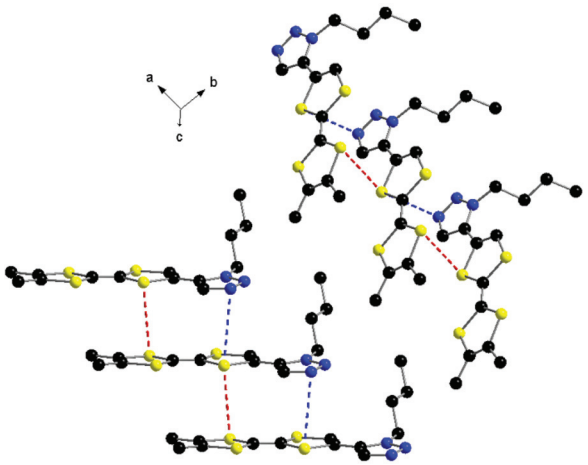

Fig. 2 Columns of donors **2** with an emphasis on the N···S and S···S intermolecular contacts. Hydrogen atoms have been omitted.

solvent from a 1 : 1 MeOH–CH_2Cl_2 solution. The compound crystallizes in the monoclinic system, space group $P2_1/c$, with one independent molecule in the unit cell. The conformation between the TTF and triazole is *s-trans* when considering the double bonds C5═C6 and C7═C8, with a very small value of 7.4° for the TTF···triazole dihedral angle (Fig. 1). The central C3═C4 bond measures 1.260(4) Å, in agreement with the neutral state of the donor.

At the supramolecular level the formation of columns is observed, in which the donors are shifted with respect to each other along the longitudinal axis in such a way that a triazole ring stacks with the TTF unit below, with N···S and S···S contacts of 3.55 and 3.72 Å, respectively (Fig. 2).

This arrangement is different to that encountered in the structure of **1**, where the formation of head-to-tail dimers was observed. The columns of **2** further interact laterally along the *c* axis through short N···S contacts and N···H_{vinyl} hydrogen bonds of 2.87 and 2.83 Å, respectively (Fig. 3). Thus, the overall supramolecular architecture results from the interplay of S···S, N···S and N···H intermolecular interactions. As a general feature of the TTF-mono(triazole) donors, when comparing the

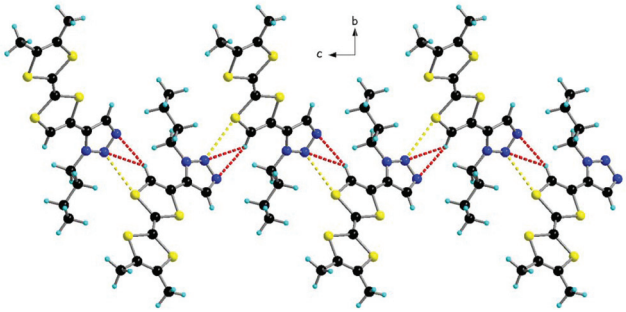

Fig. 3 Packing of **2** along the *c* axis with an emphasis on the N···S and N···H_{vinyl} interactions.

structures of **1**[7] and **2**, one can disclose the planarity of the system, suggesting conjugation between the two units.

The crystal structure of *ortho*-dimethyl-TTF-bis(1-benzyl-1,2,3-triazol-5-yl) (8)

Single crystals of **8** as orange plates were obtained by vapour diffusion of pentane into a solution of the compound in methylene chloride. The donor crystallizes in the orthorhombic system, with the non-centrosymmetric space group $P2_12_12_1$, with one independent molecule in the asymmetric unit. The most striking peculiarity in the structure is the non-planarity of the two triazole rings with respect to the TTF backbone, with dihedral angles of 87.9° and 37.0° for TTF···$triazole_{N1N2N3}$ and TTF···$triazole_{N4N5N6}$, respectively (Fig. 4). This feature is very likely due to the steric hindrance caused by the vicinity of the two heterocycles, which is comparable to the situation observed in the solid state structures of TTF-mono(oxazolines)[14a] and TTF-bis(oxazolines).[17] Moreover, the intramolecular π-stacking interaction established between the triazole N4N5N6 and the Ph ring of the other triazole unit, which are parallel at a distance of 3.4 Å, probably also contributes to the stabilization of this conformation. Bond lengths, such as the central C3═C4 bond and the internal C–S bonds, have typical values for a neutral donor (see ESI†).

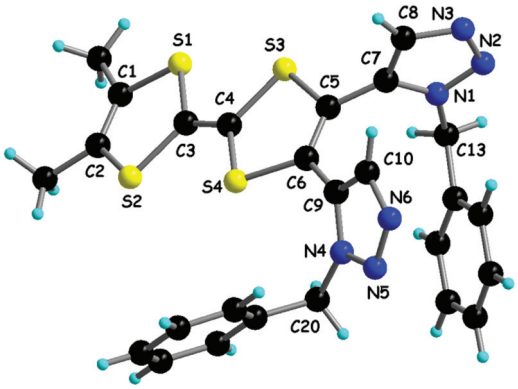

Fig. 4 Molecular structure of **8** along with the numbering scheme.

At the supramolecular level there is no short S···S intermolecular contact, very likely because of the presence of the bulky benzyl groups on TTF. However, a network of intermolecular N···H interactions develops, particularly involving the benzylic protons (see ESI†).

For the use of precursors such as the TTF-bis(triazole) **8** in electrocrystallization experiments for the preparation of radical cation salts, the replacement of the benzyl groups by less bulky substituents, *e.g.* *n*-Bu as in **2**, can be envisaged in order to allow the occurrence of TTF···TTF intermolecular interactions which are crucial for the establishment of conductivity paths. It is clear that, when analysing the structures of **1**,[7] **2** and **8**, and also the other TTF-triazole derivatives,[7] the presence of the triazole ring on TTF provides additional possibilities for intermolecular interactions such as hydrogen bonding, π–π stacking and donor–acceptor, and thus results in the emergence of original architectures. Moreover, the unsubstituted nitrogen atoms can in principle be protonated or alkylated, which should allow for the modulation of the electron donor character of TTF, the intra- and intermolecular charge transfer, and the geometry of the compound.

Protonation and alkylation studies with 1 and 8

The protonation of the mono(triazole) **1** and bis(triazole) **8**, both possessing benzyl substituents, has been monitored by UV-vis spectroscopy. As previously described, in the UV-vis spectra of TTF-triazoles, an absorption band is observed at around λ_{max} = 388–394 nm, corresponding to a partial charge transfer from TTF to triazole, as determined by TD DFT calculations.[7] In the bis(triazole) **8**, this band is centered at 415 nm (Fig. 5), with the red shift with respect to the mono(triazole) **1** being in agreement with a smaller HOMO–LUMO gap when compared to **1**. Since the oxidation of **8** occurs at a more anodic potential than the oxidation of **1**, indicating a lower energy HOMO level for **8** than for **1**, it can be concluded that the variation ΔE_{LUMO} is larger than ΔE_{HOMO} when going from **1** to **8**. The protonation or alkylation of the triazole ring is expected to increase its withdrawing character, and, consequently, result in a red shift of the charge transfer band. The stepwise addition of up to 1 equivalent of HBF_4 in a CH_2Cl_2 solution of **1** indeed leads to a red shift of the charge transfer band from 394 nm (**1**) to 422 nm ($[\mathbf{1}–H]^+BF_4^-$), with the existence of a clear isosbestic point at 416 nm (see ESI†). In the same time, practically no variation of the position of the high energy bands ranging between 250–350 nm is observed. Further addition of HBF_4 produces no further change to the spectrum, in agreement with the presence of only one

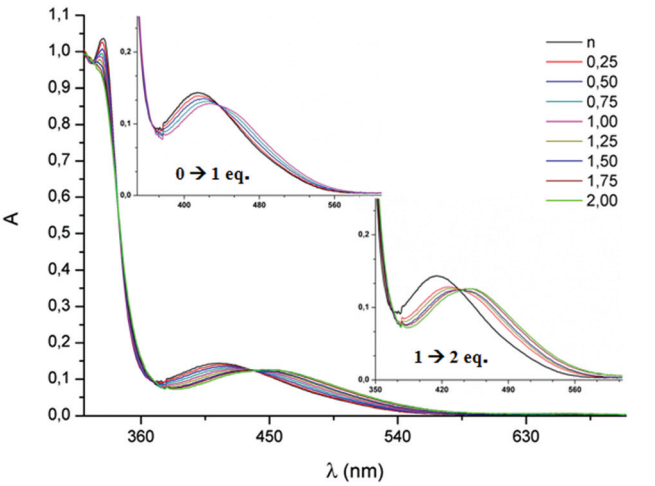

Fig. 5 UV-vis absorption spectra of **8** (10^{-4} M in CH_2Cl_2) during the stepwise addition of HBF_4; the insets magnify the charge transfer band.

basic N atom. When the same type of experiment was performed with the bis(triazole) **8**, a first bathochromic shift of 14 nm was observed by adding up to 1 equivalent of HBF_4, followed by a second shift of 22 nm between 1 and 2 equivalents of HBF_4 (Fig. 5).

In order to isolate and characterize in detail a triazolium salt, the precursor **1** was reacted with trimethyloxonium tetrafluoroborate $(Me_3O)BF_4$ to afford **9** (Scheme 4).

The triazolium salt **9** was obtained as an analytically pure brown solid, and suitable single crystals, as red blocks, were grown by the slow diffusion of diethyl ether into a solution of **9** in acetonitrile. The cyclic voltammetry measurements show anodic shifts of 0.07 and 0.06 V for the first and second oxidation potentials respectively, when compared to the neutral precursor **1** (see ESI†). In line with the observations from the protonation experiment, a large red shift of 57 nm in the UV-vis spectrum is observed for the charge transfer band which is now centred at 451 nm (see ESI†).

The final proof for the cationic structure of **9** was provided by the single crystal X-ray analysis. The compound crystallizes in the triclinic system, space group $P\bar{1}$, with one independent TTF-triazolium cation and one BF_4 anion in the asymmetric unit. As clearly observed (Fig. 6), the methylation took place at the N3 atom, which is the most nucleophilic. There is now perfect planarity between the TTF and triazolium units, while the Ph ring is perpendicular to the rest of the molecule.

The central C3═C4 bond length of 1.351(4) Å is in the normal range for a neutral donor and compares very well with

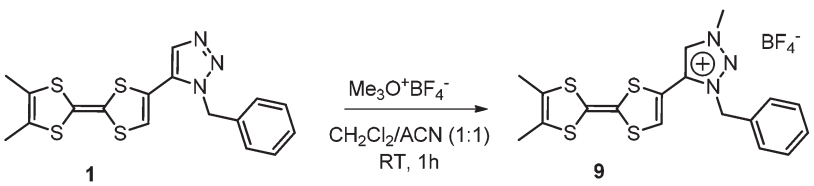

Scheme 4 Alkylation of **1**.

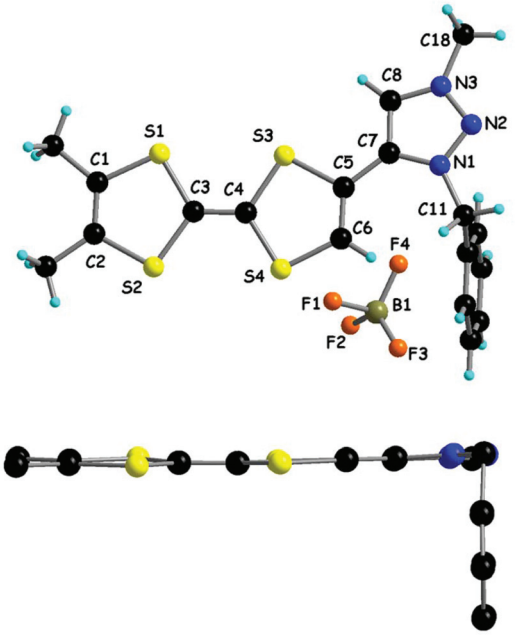

Fig. 6 Molecular structure of **9** along with the numbering scheme (up) and a lateral view of the donor molecule (bottom).

the value of 1.350(5) Å in the neutral precursor **1**. Nevertheless, the most important structural effect of the methylation concerns, as expected, the triazole ring, since in **9** the N–N distances have closer values, *i.e.* 1.326(4) Å for N1–N2 and 1.306(4) Å for N2–N3, as an effect of the conjugation, and, moreover, are shorter than the distances of 1.353(4) and 1.316(4) Å, respectively, observed in the neutral triazole. In the packing there is no short intermolecular S···S contact (see ESI†), yet hydrogen bonds of F···H-type are established between the BF_4 anions and vinylic, benzylic and NMe protons (see ESI†).

Conclusions

The synthesis of TTF-bis(triazoles) as 1,4- and 1,5-isomers was attempted following copper and ruthenium-catalyzed azide–alkyne cycloaddition reactions, respectively. The access to these bis(triazole) precursors proved to be much more problematic than the preparation of TTF-mono(triazoles), very likely because of the sensitivity of the TTF-bis(acetylene) precursor and the TTF-triazole-acetylene intermediate, since only the 1,5-isomer of the *ortho*-dimethyl-TTF-bis(triazole) could be prepared by ruthenium-based catalysis. The same reaction allowed the preparation of TTF-mono(triazoles) with benzyl or *n*-butyl substituents on the triazole ring. The substitution patterns and number of triazole units greatly influences the solid state structures of these electroactive precursors. As a general structural feature, the triazole units engage in the solid state in intermolecular π–π interactions and hydrogen bonding, thus competing with the classical TTF···TTF interactions. Modulation of the intramolecular charge transfer, TTF → triazole, was achieved by protonation of the triazole units with HBF_4, monitored by UV-visible spectroscopy. Moreover, a triazolium salt was isolated and structurally characterized by methylation with the strong electrophilic agent $(Me_3O)BF_4$. All of these TTF-triazoles and derivatives constitute valuable precursors for radical cation salts since they all possess good electron donating properties. The coordinating properties of triazoles can be also exploited, especially when associated to pyridines within chelating ligands.[18] These possibilities are actively being investigated in our laboratory.

Experimental

General

Dry THF and diethyl ether were obtained from a solvent purification system (LC Technology Solutions Incorporated). Nuclear magnetic resonance spectra were recorded on a Bruker Advance DRX 300 spectrometer operating at 300 MHz for ^1H and 75 MHz for ^{13}C. Chemical shifts are expressed in parts per million (ppm) downfield from external TMS. The following abbreviations are used: s, singlet; d, doublet; t, triplet; m, multiplet. MALDI-TOF MS spectra were recorded on a Bruker Biflex-IIITM apparatus, equipped with a 337 nm N_2 laser. Elemental analyses were recorded using a Flash 2000 Fisher Scientific Thermo Electron analyzer. IR spectra were recorded on a Bruker FT-IR Vertex 70 spectrometer equipped with a platinum diamond ATR accessory.

The compounds *ortho*-dimethyl-TTF **3**[19] and *ortho*-dimethyl-ethynyl-TTF[20] were prepared according to the published procedures.

1-Butyl-5-(*ortho*-dimethyl-tetrathiafulvalenyl)-1,2,3-triazole 2

In a Schlenk tube, *ortho*-dimethyl-ethynyl-TTF (120 mg, 0.47 mmol), *n*-butyl azide (70 mg, 0.71 mmol) and Cp*RuCl-$(PPh_3)_2$ (22 mg, 6 mol%) were dissolved in dry THF (8 mL). The reaction mixture was heated at 65 °C overnight and concentrated under vacuum. The crude product was then purified by chromatography over SiO_2 (CH_2Cl_2–AcOEt 3 : 1 as the eluent, R_f = 0.3) to yield **2** as an orange solid (130 mg, 78%). Suitable single crystals for X-ray analysis were obtained by slow evaporation of the solvent from a MeOH–CH_2Cl_2 (1 : 1) solution of **2**.

^1H NMR ($CDCl_3$ + NEt_3, 300 MHz) δ (ppm) 7.70 (s, 1H), 6.44 (s, 1H), 4.42 (t, 2H, J = 7.3 Hz), 1.99 (s, 6H), 1.91 (qt, 2H, J = 7.3 Hz), 1.37 (sext, 2H, J = 7.3 Hz), 0.98 (t, 3H, J = 7.3 Hz); $\{^1H\}^{13}C$ NMR ($CDCl_3$ + NEt_3, 75 MHz) δ (ppm) 134.2, 129.4, 123.0, 122.9, 121.1, 119.8, 113.2, 106.5, 46.2, 32.13, 19.8, 13.8, 13.5; MS (MALDI-TOF) m/z = 354.7 (M^+); Anal. calcd for $C_{14}H_{17}N_3S_4$: C, 47.29; H, 4.82; N, 11.82; S, 36.07%, found: C, 47.58; H, 4.75; N, 11.44; S, 35.83%.

2,3-Diiodo-6,7-dimethyltetrathiafulvalene 4

In a Schlenk tube, *ortho*-dimethyl-TTF **3** (600 mg, 2.58 mmol) was dissolved in dry diethyl ether (80 mL) under argon at −78 °C. Diisopropylethylamine (798 μL, 5.68 mmol), followed by butyllithium (3.55 mL, 5.68 mmol) (1.6 M solution in

hexane) were then added to the solution. The reaction mixture was stirred at −78 °C for one hour and a yellow precipitate appeared. Perfluorohexyl iodide (1.45 mL, 6.71 mmol) was added and the reaction mixture was allowed to warm up slowly to room temperature and was stirred overnight. After evaporation of the solvent, the crude product was purified by chromatography over SiO_2 (cyclohexane–CS_2 1 : 1 as the eluent, R_f = 0.8), yielding **4** as a light red solid (662 mg, 53%).

^{1}H NMR ($CDCl_3$ + NEt_3, 300 MHz) δ (ppm) 2.00 (s, 6H); $\{^1H\}^{13}$C NMR ($CDCl_3$ + NEt_3, 75 MHz) δ (ppm) 128.4, 128.3, 122.9, 114.5, 111.4, 77.2, 13.8; MS (MALDI-TOF) m/z = 483.7 (M^+); Anal. calcd for $C_8H_6I_2S_4$: C, 19.84; H, 1.25; S, 26.49%, found: C, 20.66; H, 1.30; S, 26.54%.

2,3-Di(trimethylsilylethynyl)-6,7-dimethyltetrathiafulvalene 5

In a Schlenk tube, **4** (500 mg, 1.03 mmol), $Pd(PPh_3)_4$ (60 mg, 5 mol%) and CuI (20 mg, 10 mol%) were dissolved in dry THF (15 mL). Diisopropylamine (871 μL, 6.20 mmol) and trimethylsilylacetylene (882 μL, 6.20 mmol) were then added to the solution. The reaction mixture was heated at 60 °C overnight under argon. After evaporation of the solvent, the crude product was purified by chromatography over SiO_2 (cyclohexane as the eluent), yielding **5** as a purple solid (377 mg, 86%). Suitable single crystals for X-ray analysis were obtained by the recrystallization of **5** in acetonitrile.

^{1}H NMR ($CDCl_3$ + NEt_3, 300 MHz) δ (ppm) 1.97 (s, 6H), 0.25 (s, 18H); $\{^1H\}^{13}$C NMR ($CDCl_3$ + NEt_3, 75 MHz) δ (ppm) 125.8, 122.7, 122.0, 114.0, 106.5, 99.7, 94.9, 13.8, −0.29; MS (MALDI-TOF) m/z = 424.0 (M^+); Anal. calcd for $C_{18}H_{24}S_4Si_2$: C, 50.89; H, 5.69; S, 30.19%, found: C, 51.21; H, 5.75; S, 30.05%.

2,3-Di(ethynyl)-6,7-dimethyltetrathiafulvalene 6

To a degassed solution of **5** (150 mg, 0.35 mmol) in THF–methanol (20 mL, 1 : 1 v/v), tetrabutylammonium fluoride (850 μL, 0.85 mmol) (1 M solution in THF) was added. The reaction mixture was stirred at RT for 45 min and then the solvents were removed under vacuum. The crude product was then purified by flash chromatography over neutral alumina (CH_2Cl_2 as the eluent) to yield **6** as a light purple solid (70 mg, 71%) which was directly engaged in the next step.

^{1}H NMR ($CDCl_3$ + NEt_3, 300 MHz) δ (ppm) 3.44 (s, 2H), 2.00 (s, 6H).

ortho-Dimethyl-TTF-2′-(*N*-benzyl-1,2,3-triazol-5-yl)-3′-ethynyl 7

In a Schlenk tube, **6** (70 mg, 0.25 mmol), benzyl azide (90 mg, 0.75 mmol) and CuI (5.7 mg, 6 mol%) were dissolved in $CHCl_3$ (5 mL) and *N*,*N*-diisopropylethylamine (3 mL). The reaction mixture was heated at 65 °C overnight and concentrated under vacuum. The crude product was then purified by chromatography over SiO_2 (CH_2Cl_2–AcOEt 3 : 1, and a few drops of NEt_3 as the eluent, R_f = 0.4) to yield **7** as an orange solid (10 mg, 10%).

^{1}H NMR ($CDCl_3$ + NEt_3, 300 MHz) δ (ppm) 8.16 (s, 1H), 7.44–7.39 (m, 3H), 7.30 (m, 2H), 5.60 (s, 2H), 3.61 (s, 1H), 1.98 (s, 6H); MS (MALDI-TOF) m/z = 413.2 (M^+).

ortho-Dimethyl-TTF-bis(1-benzyl-1,2,3-triazol-5-yl) 8

In a Schlenk tube, **6** (120 mg, 0.28 mmol), benzyl azide (112 mg, 0.85 mmol) and $Cp^*RuCl(PPh_3)_2$ (14 mg, 6 mol%) were dissolved in dry THF (8 mL). The reaction mixture was heated for 24 h at 65 °C and concentrated under vacuum. The crude product was then purified by chromatography over SiO_2 (CH_2Cl_2–AcOEt 1 : 1 as the eluent) to yield **8** as a beige solid (35 mg, 15%). Suitable single crystals for X-ray analysis were grown by vapour diffusion of pentane onto a CH_2Cl_2 solution of **8**.

^{1}H NMR ($CDCl_3$ + NEt_3, 300 MHz) δ (ppm) 7.43–7.37 (m, 6H), 7.30–7.26 (m, 4H), 6.54 (s, 2H), 5.41 (s, 4H), 2.08 (s, 6H); $\{^1H\}^{13}$C NMR ($CDCl_3$ + NEt_3, 75 MHz) δ (ppm) 134.6, 134.5, 129.0, 128.9, 128.2, 127.2, 123.1, 121.7, 117.7, 65.7, 13.6; MS (MALDI-TOF) m/z = 545.2 (M^+); Anal. calcd for $C_{26}H_{22}N_6S_4$: C, 57.12; H, 4.06; N, 15.37; S, 23.46%, found: C, 56.86; H, 4.20; N, 14.43; S, 21.96%.

1-Benzyl-3-methyl-5-(6′,7′-dimethyltetrathiafulvalenyl)-1,2,3-triazolium·BF_4 9

In a Schlenk tube, **1** (35 mg, 0.09 mmol) was dissolved in a 6 mL mixture of acetonitrile–dichloromethane (1 : 1). Then, trimethyloxonium tetrafluoroborate (13.3 mg, 0.09 mmol) dissolved in acetonitrile (3 mL) was added and the solution, which turned darker, was stirred for 1 h at room temperature. Diethyl ether (10 mL) was added to the reaction mixture, and the precipitate formed was filtered and washed with cold dichloromethane and diethyl ether to yield **9** as a brown solid (31 mg, 77%). Suitable single crystals for X-ray analysis were grown by the slow diffusion of diethyl ether into an acetonitrile solution of **9**.

^{1}H NMR (DMSO, 300 MHz) δ (ppm) 9.19 (s, 1H), 7.48–7.40 (m, 4H), 7.38–7.31 (m, 2H), 5.93 (s, 2H), 4.32 (s, 3H), 1.99 (s, 6H); $\{^1H\}^{13}$C NMR (DMSO, 75 MHz) δ (ppm) 134.1, 132.5, 132.3, 130.6, 129.6, 129.5, 128.9, 123.5, 113.9, 113.1, 104.7, 55.5, 13.9; MS (MALDI-TOF) m/z = 403.8 (M^+); Anal. calcd for $C_{18}H_{18}BF_4N_3S_4$: C, 43.99; H, 3.69; N, 8.55; S, 26.10%, found: C, 44.38; H, 3.96; N, 8.26; S, 25.68%.

X-Ray structure determination

Details of the data collection and solution refinement are given in Table 1 (see also ESI† for **5**). X-ray diffraction measurements were performed on a Bruker Kappa CCD diffractometer, operating with a Mo Kα (λ = 0.71073 Å) X-ray tube with a graphite monochromator. The structures were solved (SHELXS-97) by direct methods and refined (SHELXL-97) by full matrix least-square procedures on F^2.[21] All of the non-hydrogen atoms were refined anisotropically. Hydrogen atoms were introduced at calculated positions (riding model) and included in structure factor calculations, but not refined. Crystallographic data for the four structures have been deposited with the Cambridge Crystallographic Data Centre, with the deposition numbers CCDC 982420 (**2**), CCDC 982421 (**5**), CCDC 982422 (**8**) and CCDC 982423 (**9**).

Table 1 Crystal data and structure refinement for **2**, **8** and **9**

Compound	**2**	**8**	**9**
Empirical formula	$C_{14}H_{17}N_3S_4$	$C_{26}H_{22}N_6S_4$	$C_{18}H_{18}BF_4N_3S_4$
fw	355.55	546.74	491.40
T (K)	293(2)	293(2)	293(2)
Wavelength (Å)	0.71073	0.71073	0.71073
Crystal system	Monoclinic	Orthorhombic	Triclinic
Space group	$P2_1/c$	$P2_12_12_1$	$P\bar{1}$
Unit cell dimensions			
a (Å)	5.3381 (5)	6.7025 (5)	9.7854 (6)
b (Å)	25.844 (19)	19.621 (2)	11.173 (7)
c (Å)	11.069 (10)	20.267 (3)	11.332 (5)
α (°)	90.00	90.00	70.909 (4)
β (°)	99.56 (7)	90.00	81.108 (4)
γ (°)	90.00	90.00	68.833 (4)
V (Å^3)	1505.9 (2)	2665.3 (6)	1090.88 (11)
Z	4	4	2
D_c (g cm^{-3})	1.568	1.363	1.496
Abs coeff (mm^{-1})	0.626	0.384	0.480
F(000)	744	1136	504
Crystal size (mm^3)	0.6 × 0.1 × 0.1	0.6 × 0.3 × 0.08	0.8 × 0.4 × 0.4
θ range for data collection (°)	3.15–27.50	2.71–24.03	2.35–27.00
Limiting indices	$-6 \le h \le 6$, $-33 \le k \le 32$, $-14 \le l \le 14$	$-7 \le h \le 7$, $-22 \le k \le 21$, $-23 \le l \le 20$	$-12 \le h \le 12$, $-14 \le k \le 14$, $-14 \le l \le 14$
Reflections collected	17 019	13 973	21 173
Independent reflections	3380	4058	4719
Completeness (%) to θ = 25.59°	98.1	98.1	98.9
Abs correction	Multi-scan	Multi-scan	Multi-scan
Refinement method	Full-matrix least squares on F^2	Full-matrix least squares on F^2	Full-matrix least squares on F^2
Data/restraints/parameters	3380/0/190	4058/0/325	4719/0/271
GOF on F^2	1.011	1.125	1.132
Final R indices [$I > 2\sigma(I)$]	R_1 = 0.0579, wR_2 = 0.1453	R_1 = 0.0482, wR_2 = 0.0789	R_1 = 0.0657, wR_2 = 0.2094
R indices (all data)	R_1 = 0.1176, wR_2 = 0.1640	R_1 = 0.0876, wR_2 = 0.0923	R_1 = 0.0804, wR$_2$ = 0.2255
Largest diff. peak and hole (e Å^{-3})	0.393 and −0.302	0.196 and −0.172	1.328 and −0.768

Acknowledgements

This work was supported by the CNRS, University of Angers and the Ministry of Education and Research (grant to T.B.). I. Freuze and C. Mézière are thanked for the MS analyses.

References

1 (*a*) H. C. Kolb, M. G. Finn and K. B. Sharpless, *Angew. Chem., Int. Ed.*, 2001, **40**, 2004; (*b*) J. E. Moses and A. D. Moorhouse, *Chem. Soc. Rev.*, 2007, **36**, 1249.

2 (*a*) V. V. Rostovtsev, L. G. Green, V. V. Fokin and K. B. Sharpless, *Angew. Chem., Int. Ed.*, 2002, **41**, 2596; (*b*) C. W. Tornøe, C. Christensen and M. Meldalb, *J. Org. Chem.*, 2002, **67**, 3057; (*c*) J. E. Hein and V. V. Fokin, *Chem. Soc. Rev.*, 2010, **39**, 1302.

3 (*a*) Y. H. Lau, P. J. Rutledge, M. Watkinson and M. H. Todd, *Chem. Soc. Rev.*, 2011, **40**, 2848; (*b*) J. J. Bryant and U. H. F. Bunz, *Chem. - Asian J.*, 2013, **8**, 1354.

4 D. S. Pedersen and A. Abell, *Eur. J. Org. Chem.*, 2011, 2399.

5 (*a*) R. Bronisz, *Inorg. Chem.*, 2005, **44**, 4463; (*b*) B. M. J. M. Suijkerbuijk, B. N. H. Aerts, H. P. Dijkstra, M. Lutz, A. L. Spek, G. van Koten and R. J. M. K. Gebbink, *Dalton Trans.*, 2007, 1273; (*c*) M. L. Gower and J. D. Crowley, *Dalton Trans.*, 2010, **39**, 2371; (*d*) J. D. Crowley and E. L. Gavey, *Dalton Trans.*, 2010, **39**, 4035; (*e*) H. Struthers, T. L. Mindt and R. Schibli, *Dalton Trans.*, 2010, **39**, 675; (*f*) D. Schweinfurth, J. Krzystek, I. Schapiro, S. Demeshko, J. Klein, J. Telser, A. Ozarowski, C.-Y. Su, F. Meyer, M. Atanasov, F. Neese and B. Sarkar, *Inorg. Chem.*, 2013, **52**, 6880.

6 (*a*) L. Zhang, X. Chen, P. Xue, H. H. Y. Sun, I. D. Williams, K. B. Sharpless, V. V. Fokin and G. Jia, *J. Am. Chem. Soc.*, 2005, **127**, 15998; (*b*) B. C. Boren, S. Narayan, L. K. Rasmussen, L. Zhang, H. Zhao, Z. Lin, G. Jia and V. V. Fokin, *J. Am. Chem. Soc.*, 2008, **130**, 8923.

7 T. Biet, T. Cauchy and N. Avarvari, *Chem. - Eur. J.*, 2012, **18**, 16097.

8 Y.-L. Zhao, W. R. Dichtel, A. Trabolsi, S. Saha, I. Aprahamian and J. F. Stoddart, *J. Am. Chem. Soc.*, 2008, **130**, 11294.

9 K. Qvortrup, M. Å. Petersen, T. Hassenkam and M. B. Nielsen, *Tetrahedron Lett.*, 2009, **50**, 5613.

10 B.-T. Zhao, L.-W. Liu, X.-C. Li, G.-R. Qu, E. Belhadj, F. Le Derf and M. Sallé, *Tetrahedron Lett.*, 2013, **54**, 23.

11 (*a*) D. Lorcy, N. Bellec, M. Fourmigué and N. Avarvari, *Coord. Chem. Rev.*, 2009, **253**, 1398; (*b*) M. Shatruk and L. Ray, *Dalton Trans.*, 2010, **39**, 11105.

12 (*a*) E. Coronado and P. Day, *Chem. Rev.*, 2004, **104**, 5419; (*b*) L. Ouahab and T. Enoki, *Eur. J. Inorg. Chem.*, 2004, 933; (*c*) F. Riobé and N. Avarvari, *Coord. Chem. Rev.*, 2010, **254**, 1523.

13 (*a*) C. Réthoré, I. Suisse, F. Agbossou-Niedercorn, E. Guillamón, R. Llusar, M. Fourmigué and N. Avarvari, *Tetrahedron*, 2006, **62**, 11942; (*b*) C. Réthoré, F. Riobé, M. Fourmigué, N. Avarvari, I. Suisse and F. Agbossou-Niedercorn, *Tetrahedron: Asymmetry*, 2007, **18**, 1877.

14 (*a*) C. Réthoré, M. Fourmigué and N. Avarvari, *Chem. Commun.*, 2004, 1384; (*b*) C. Réthoré, M. Fourmigué and N. Avarvari, *Tetrahedron*, 2005, **61**, 10935; (*c*) A. M. Madalan, C. Réthoré and N. Avarvari, *Inorg. Chim. Acta*, 2007, **360**, 233.

15 (*a*) W. Liu, J. Xiong, Y. Wang, X.-H. Zhou, R. Wang, J.-L. Zuo and X.-Z. You, *Organometallics*, 2009, **28**, 755; (*b*) M. Nihei, N. Takahashi, H. Nishikawa and H. Oshio, *Dalton Trans.*, 2011, **40**, 2154; (*c*) G.-N. Li, Y. Liao, T. Jin and Y.-Z. Li, *Inorg. Chem. Commun.*, 2013, **35**, 27.

16 (*a*) T. Murata, Y. Morita, K. Fukui, K. Sato, D. Shiomi, T. Takui, M. Maesato, H. Yamochi, G. Saito and K. Nakasuji, *Angew. Chem., Int. Ed.*, 2004, **43**, 6343;

(*b*) J. Wu, N. Dupont, S.-X. Liu, A. Neels, A. Hauser and S. Decurtins, *Chem. - Asian J.*, 2009, **4**, 392; (*c*) T. Murata, Y. Yamamoto, Y. Yakiyama, K. Nakasuji and Y. Morita, *Bull. Chem. Soc. Jpn.*, 2013, **86**, 927.

17 F. Riobé and N. Avarvari, *Chem. Commun.*, 2009, 3753.

18 (*a*) J. D. Crowley, P. H. Bandeen and L. R. Hanton, *Polyhedron*, 2010, **29**, 70; (*b*) P. M. Guha, H. Phan, J. S. Kinyon, W. S. Brotherton, K. Sreenath, J. T. Simmons, Z. Wang, R. J. Clark, N. S. Dalal, M. Shatruk and L. Zhu, *Inorg. Chem.*, 2012, **51**, 3465; (*c*) L. Jiang, Z. Wang, S.-Q. Bai and T. S. A. Hor, *CrystEngComm*, 2013, **15**, 10451; (*d*) J. P. Byrne, J. A. Kitchen, O. Kotova, V. Leigh, A. P. Bell, J. J. Boland, M. Albrecht and T. Gunnlaugsson, *Dalton Trans.*, 2014, **43**, 196.

19 F. Gerson, A. Lamprecht and M. Fourmigué, *J. Chem. Soc., Perkin Trans. 2*, 1996, 1409.

20 C. Goze, S.-X. Liu, C. Leiggener, L. Sanguinet, E. Levillain, A. Hauser and S. Decurtins, *Tetrahedron*, 2008, **64**, 1345.

21 G. M. Sheldrick, *Programs for the Refinement of Crystal Structures*, University of Göttingen, Göttingen, Germany, 1996.